

José Romo, Alejandro Pérez-Caldentey, Manuel Cuadrado

High-speed Railway Bridges

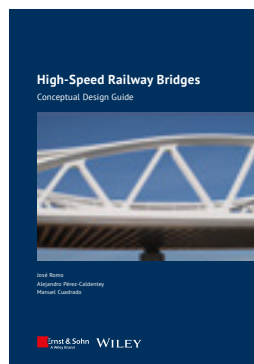
Conceptual Design Guide

- the book provides first-hand experience
- with worked calculation examples
- numerous practical examples

The need for large-scale bridges is constantly growing worldwide with the expansion of transport infrastructures. This book deals with all aspects referring to the structural conceptual design of HSR bridges taking into account the issues of track construction. With examples.

Ernst & Sohn
A Wiley Brand

WILEY



9 / 2023 ·
336 pages · 110 figures · 28 tables

Hardcover
ISBN 978-3-433-03313-5 € 109*

eBundle (Print + ePDF)
ISBN 978-3-433-03381-4 € 169*

WILEY **Ernst & Sohn**
A Wiley Brand

ABOUT THE BOOK

The need for large-scale bridges is constantly growing worldwide as the expansion of transport infrastructures with rail roads and high-speed lines is an important current task in many regions. This book develops all aspects referring to the structural conceptual design and analysis that are taken into account when planning a bridge or viaduct for a high-speed rail line. That includes the characteristics of the railway traffic such as speeds actions, limit states etc., and a detailed analysis of the superstructure of the track with its various components and singular elements. One of the special features of the book is that it not only highlights the bridge typologies and structural components related to the bridge design but also takes into account the issues of the track construction. The design basis the requirements from different situations and solutions are given.

Special attention is paid to the interactions between the structure and the track and to the dynamic nature of railway actions studying the dynamic response of the structure and its influence on the behaviour of the track and its components as well as on safety traffic flow quality and maintenance needs. The particulars of the design of high-speed rail bridges located in seismic areas are included as well. Numerous examples in all chapters serve the book's character as a useful guide to HSR bridge design and to prevent typical problems and errors.

Quantity	ISBN / Order-No.	Title	Price €
	978-3-433-03313-5	High-speed Railway Bridges	€ 109*
	978-3-433-03381-4	High-speed Railway Bridges (Print + ePDF)	€ 169*

ORDER

+49 (0)30 470 31-236

marketing@ernst-und-sohn.de

www.ernst-und-sohn.de/3313

* All book prices inclusive VAT.

Private Business

Please send your order to:
marketing@ernst-und-sohn.de

Company Abteilung	VAT-ID	
Name	Phone	Fax
Street, No.		
Zip code / City / Country	E-Mail	

www.ernst-und-sohn.de/3313

Date, Signature

. As of 8/2023

Contents

Foreword	<i>xv</i>
About the Authors	<i>xvii</i>
Acknowledgements	<i>xix</i>

1	Introduction to High-Speed Railway Bridges	1
	<i>José Romo</i>	
1.1	Book's Content	1
1.2	What is Special About a High-Speed Rail Bridge?	2
1.2.1	Dynamic Amplification and Resonance	2
1.2.2	Rail Traffic Security	3
1.2.3	Passenger's Comfort	3
1.2.4	Track–Structure Interaction	4
1.3	General Ideas on High-Speed Railway Bridges	4
1.4	Evolution and Trends in High-Speed Bridge Design	6
1.4.1	First High-Speed Bridges	6
1.4.1.1	First-Generation German Bridges	6
1.4.1.2	First-Generation French Bridges	8
1.4.1.3	First-Generation Spanish Bridges	8
1.4.2	Recent High-Speed Bridges	9
1.4.2.1	Recent French Bridges	9
1.4.2.2	Second-Generation German Bridges	9
1.4.2.3	Recent Spanish HSRB	10
1.4.2.4	Bridges for High-Speed Railway Lines in China	10
1.4.2.5	British High-Speed Bridges	12
1.4.2.6	High-Speed Railway Bridges in the USA	12
1.4.3	Conclusions	12
1.4.3.1	Viaducts	13
1.4.3.2	Long-Span Bridges	13
1.5	The Landscape and the Design of High-Speed Railway Bridges	13
1.5.1	The Traveller's Experience	13
1.5.2	The Bridge in the Landscape	15
1.5.2.1	Long Viaducts with Low Vertical Level	16
1.5.2.2	Long Viaducts with Medium or High Level	16

1.6	Railway Bridges as Landmarks or Icons of a Line	22
1.7	Railway Bridge's Legacy	23
1.8	Building for the 21st Century	24
1.9	Conclusions	24
	References	25
2	Track for High-Speed Bridges	29
	<i>Manuel Cuadrado</i>	
2.1	Introduction	29
2.2	Specific Criteria for Railway Bridges	29
2.2.1	General Criteria	29
2.2.2	Specific Criteria for High-Speed Bridges	31
2.3	Description of the Track Superstructure	31
2.3.1	Track Components: Definitions, Functions, and Qualities	32
2.3.1.1	Ballast	32
2.3.1.2	Sleepers	32
2.3.1.3	Fasteners	33
2.3.1.4	Rails	33
2.3.1.5	Switches and Crossings	34
2.3.2	Most Important Conceptual Improvements	35
2.3.2.1	Continuous Welded Rail (CWR)	35
2.3.2.2	Track–Infrastructure Interaction: Better Understanding	36
2.3.3	Evolution of the Different Components	36
2.3.3.1	Ballast	36
2.3.3.2	Sleepers	37
2.3.3.3	Fastenings	39
2.3.3.4	Rails	40
2.3.4	Track Options Currently Available for High Speed	41
2.3.4.1	Optimised Ballasted Track	41
2.3.4.2	New Ballastless Track	43
2.4	SLS Related to the Track	44
2.4.1	Dynamic Interaction: Track–Vehicle	44
2.4.2	Track Geometry Quality	46
2.4.3	SLS Verifications Regarding Deformations and Vibrations	48
2.4.3.1	Criteria for Traffic Safety	48
2.4.3.2	Comfort Criteria	55
	References	57
3	Conceptual Design of High-Speed Railway Bridges	61
	<i>José Romo</i>	
3.1	Introduction	61
3.2	Structural and Functional Specific Requirements for High-Speed Railway Bridges	62
3.2.1	Introduction	62
3.2.2	Control of Vertical Acceleration	62

3.2.3	Rotation at Expansion Joints	62
3.2.4	Horizontal Braking and Traction Forces and Relative Movements Between Deck and Infrastructure	62
3.2.5	Track-Bridge Deck Interaction	63
3.2.6	Expansion Joints	63
3.3	Longitudinal Design Strategies	64
3.3.1	General Concepts	64
3.3.2	Ballasted Track	65
3.3.3	Ballastless Track	66
3.3.4	Actions to be Considered at the Fixed Point	66
3.4	Design Situation of High-Speed Railway Bridges	66
3.4.1	Short Crossing at Low Level	67
3.4.2	Long Structures	67
3.4.2.1	Low Profile	68
3.4.3	High-Level Viaducts	71
3.4.4	Long Span Structures	72
3.5	Structural Types	72
3.5.1	Straight Deck Solutions	72
3.5.1.1	Simply Supported Deck	72
3.5.1.2	Continuous Slab Concrete Decks	73
3.5.1.3	Precast Beam Decks	74
3.5.1.4	Concrete Box Hollow Sections	78
3.5.1.5	Steel Beam Decks	80
3.5.1.6	Steel Semi-through Decks	81
3.5.2	Truss Bridges	82
3.5.3	Arch Bridges	83
3.5.3.1	Upper Deck Bridges	83
3.5.3.2	Tied Arch Bridges	85
3.5.4	Cable-Supported Bridges	85
3.5.4.1	Extradosed Bridges	85
3.5.4.2	Cable-Stayed Bridges	86
3.5.4.3	Suspension Bridges	88
3.5.4.4	Hybrid Bridges	89
3.6	Structural Elements – Substructure	89
3.6.1	Abutments	90
3.6.1.1	Abutments with Expansion Joint in Structure Only	90
3.6.1.2	Abutments with Expansion Joint in Structure and Track	90
3.6.1.3	Fixed Abutments	91
3.6.2	Piers	95
3.6.3	Bearings	95
3.6.3.1	General Bearing Layout	96
3.7	Seismic Design	99
3.7.1	Seismic Design Strategies	99
3.7.2	Seismic Behaviour and Deck Articulation	99
3.7.3	Longitudinal Behaviour	100

3.7.3.1	Simply Supported Spans	100
3.7.3.2	Continuous Deck	100
3.7.4	Transversal Behaviour	101
3.7.4.1	Introduction	101
3.7.4.2	Fixed Transversal Support	101
3.7.4.3	Transversal Damping Systems	102
3.7.4.4	Damping Devices Plus Bearings	104
3.8	Worked Example	106
3.8.1	Introduction: Aim and Data	106
3.8.1.1	Topography	106
3.8.1.2	Plan and Elevation	106
3.8.1.3	Railway Platform Section – Project Speed	106
3.8.1.4	Water Flood Level	107
3.8.1.5	Preliminary Geotechnical Data	107
3.8.2	Methodology	107
3.8.3	Critical Analysis of Existing Information	107
3.8.4	Determination of the Length of the Viaduct, Selection of the Fixed Point	108
3.8.5	Span Distribution	109
3.8.6	Deck Pre-dimensioning	109
3.8.7	Pre-design of the Infrastructure	112
3.8.7.1	Fixed Point	112
3.8.7.2	Bearings	112
3.8.7.3	Abutments	112
3.8.7.4	Piers	113
	References	115
4	Design Basis	117
	<i>José Romo</i>	
4.1	Introduction	117
4.2	Design Situations	117
4.3	Rail Traffic Actions and Other Actions Specific of Railway Bridges	118
4.3.1	Permanent Loads	118
4.3.1.1	Self-Weight	118
4.3.1.2	Dead Loads	118
4.3.1.3	Partial Ballast Removal	119
4.3.2	Variable Loads	119
4.3.2.1	Vertical Live Loads	119
4.3.2.2	Traction and Braking Forces	121
4.3.2.3	Centrifugal Forces	122
4.3.2.4	Nosing Forces	123
4.3.2.5	Aerodynamic Actions from Passing Trains	123
4.3.2.6	Thermal Actions	123
4.3.2.7	Bearing Friction	124
4.3.3	Dynamics Effects	124

4.3.3.1	Introduction	124
4.3.3.2	Consideration of Dynamic Effects	125
4.3.4	Railway Vehicle Derailment	125
4.3.4.1	Railway Vehicle Impacts	125
4.4	Application of Traffic Loads on Railway Bridges	126
4.4.1	General	126
4.4.1.1	Load Situations for Structural Design	127
4.4.1.2	Load Situations for Limit State and Associated Acceptance Criteria	127
4.4.2	Groups of Loads	127
4.4.2.1	Characteristic Values of Multicomponent Action	127
4.5	Traffic Loads for Fatigue	128
4.6	Verifications Regarding Deformation and Vibrations for Railway Bridges	128
4.7	Worked Example	129
4.7.1	Introduction	129
4.7.1.1	Calculation of Reactions at Bearings: Pre-dimensioning	130
4.7.1.2	Calculation of Forces and Preliminary Design of the Fixed Abutment	130
4.7.2	Actions	130
4.7.2.1	Vertical Loads	130
4.7.2.2	Horizontal Forces	131
4.7.2.3	Wind Speed	132
4.7.3	Calculation of Reactions at Bearings: Pre-dimensioning	133
4.7.3.1	Vertical Forces	133
4.7.3.2	Centrifugal Forces	134
4.7.3.3	Wind at Unloaded State	135
4.7.3.4	Wind with Live Load	135
4.7.3.5	Reactions in Pier Heads	135
4.7.3.6	Transversal Wind Bearings Reactions	136
4.7.3.7	Loads per Bearings	136
4.7.4	Fixed Abutment Loads	137
4.7.4.1	Introduction	137
4.7.4.2	Loads Transmitted by the Deck	137
4.7.4.3	Forces Acting on the Abutment	138
	References	140
5	Dynamic Behaviour of High-Speed Railway Bridges	143
	<i>Alejandro Pérez-Caldentey</i>	
5.1	Introduction	143
5.1.1	Resonance	143
5.1.2	Envelope Dynamic Factor	144
5.1.3	Dynamic Factor for Real Trains Obtained by Means of Analytical Formulations	145
5.1.4	Dynamic Factor Obtained by Dynamic Analysis	147

5.2	Methods for Dynamic Calculations and Structural Response	153
5.2.1	Modal Superposition	153
5.2.1.1	Matrix Formulation for Finite Element Analysis	153
5.2.1.2	Formulation Based on Assumed Eigenforms	155
5.2.2	Response to the Isolated Load	158
5.2.3	Response to the Train Loads	162
5.2.4	Effect of Damping	164
5.2.5	Dynamic Interaction Between Vehicle and Structure	165
5.3	Interoperability	167
5.3.1	Introduction	167
5.3.2	Universal Dynamic Train A	167
5.3.3	Universal Dynamic Train B	167
5.4	Application Examples	168
5.4.1	Case Without Dynamic Analysis	168
5.4.2	Case with Dynamic Analysis	169
	References	183
6	Longitudinal Track–Structure Interaction	185
	<i>Manuel Cuadrado and Alejandro Pérez-Caldentey</i>	
6.1	Introduction	185
6.2	Problem Statement	185
6.3	Model for Analysis	188
6.3.1	General Considerations	188
6.3.1.1	Rails	189
6.3.1.2	Deck	189
6.3.1.3	Interaction Between Rails and Track Base	189
6.3.1.4	Bearings	189
6.3.1.5	Columns	190
6.3.1.6	Foundations	190
6.4	Actions	191
6.4.1	Temperature Variations	191
6.4.1.1	Case Without Track Joint	191
6.4.1.2	Case with Track Joint	191
6.4.2	Traction and Braking Forces	191
6.4.3	Vertical Loads	192
6.4.4	Creep and Shrinkage	192
6.4.5	Combination of Actions	193
6.5	Verifications	194
6.5.1	Verifications in Terms of Stresses	194
6.5.2	Verifications in Terms of Displacements	195
6.5.3	Criteria for Placing a Track Joint	196
6.6	Rail Expansion Joints	197
6.6.1	Design of REJs – Calculation of the Maximum Displacement	197
6.6.2	Regulation	201
6.6.3	Installation	201
6.7	Longitudinal Schemes	203

6.7.1	Continuous Deck with a Single Fixed Point Located at One of the Abutments	203
6.7.1.1	General	203
6.7.1.2	Examples	204
6.7.2	Continuous Deck with the Fixed Point Located on One of the Central Piers	211
6.7.2.1	General	211
6.7.3	Simply Supported Spans Without Longitudinal Continuity, with a Fixed Point on Each Span	211
6.7.3.1	General	211
6.7.3.2	Example	212
6.7.4	Fixed Points at the Two Abutments and a Structural Joint in the Middle	212
6.7.4.1	General	212
6.7.4.2	Example	214
6.7.5	Deck Divided into Several Continuous Stretches, Each One Including Several Spans and One Fixed Point	216
6.7.5.1	General	216
6.7.5.2	Example	217
6.7.6	Especial Situations	218
6.7.6.1	Seismic Design	218
6.7.6.2	Exceptional Geometries	226
6.7.6.3	Example of Exceptional Geometry	226
6.8	Example of Track–Structure Interaction	229
6.8.1	Verification of Stresses in the Rails	229
6.8.2	Verification of Horizontal Displacement at Abutment 2 Due to Braking and Traction Forces	231
6.8.3	Verification of Horizontal Displacement at Abutment 2 Due to Vertical Train Loads	232
6.8.4	Verification of Vertical Displacement at Abutment 2 Due to Vertical Train Loads and Temperature Variations	234
	References	235
7	Conceptual Design for Maintenance	239
	<i>José Romo</i>	
7.1	Introduction	239
7.2	Accesses	240
7.2.1	Decks	240
7.2.2	Piers	240
7.2.3	Abutments	241
7.3	Bearings	242
7.4	Expansion Joints	243
7.5	Drainage	246
7.6	Conclusions	248
	References	248

Appendix A Basic Concepts of Dynamics 249*Alejandro Pérez-Caldentey*

- A.1 Dynamics of Single Degree-of-Freedom Systems 249
- A.1.1 Dynamic Response to Moving Loads (Dynamic Load Factor) 249
- A.1.2 Basics of Resonance 257
- A.1.3 Solution of the Equation of Motion of a SDOF Damped System Subjected to a Triangular Load 258
- A.1.3.1 Auxiliary Expressions – Integrals I_1 , I_2 , and Their Derivatives 259
- A.1.3.2 Solution for the damped SDOF System Subjected to a Triangular Load 261
- Reference 262

Appendix B Singular Bridges for High-Speed Railway Lines 263*José Romo*

- B.1 Germany 263
- B.1.1 Gemünden Bridge 264
- B.1.1.1 Data Summary 264
- B.1.1.2 Description 264
- Further Reading 264
- B.1.2 Veitshöchheim Bridge 266
- B.1.2.1 Data Summary 266
- B.1.2.2 Description 266
- Further Reading 266
- B.1.3 Pfeiffetal Bridge 268
- B.1.3.1 Data Summary 268
- B.1.3.2 Description 268
- Further Reading 268
- B.1.4 Nantenbach Bridge 270
- B.1.4.1 Data Summary 270
- B.1.4.2 Description 270
- Further Reading 270
- B.1.5 Unstruttal Bridge 272
- B.1.5.1 Data Summary 272
- B.1.5.2 Description 272
- Further Reading 272
- B.1.6 Gänsebachtal Viaduct 274
- B.1.6.1 Data Summary 274
- B.1.6.2 Description 274
- Further Reading 274
- B.1.7 Hämerten Bridge 276
- B.1.7.1 Data Summary 276
- B.1.7.2 Description 276
- Further Reading 276
- B.1.8 Filstal Bridge 278
- B.1.8.1 Data Summary 278

- B.1.8.2 Description 278
 - Further Reading 278
- B.2 France 281
 - B.2.1 Garde-Adhémar Viaduct 282
 - B.2.1.1 Data Summary 282
 - B.2.1.2 Description 282
 - Further Reading 282
 - B.2.2 Avignon Viaducts 284
 - B.2.2.1 Data Summary 284
 - B.2.2.2 Description 284
 - Further Reading 284
 - B.2.3 Mornas Viaduct 286
 - B.2.3.1 Data Summary 286
 - B.2.3.2 Description 286
 - Further Reading 286
 - B.2.4 Savoureuse Viaduct 288
 - B.2.4.1 Data Summary 288
 - B.2.4.2 Description 288
 - Further Reading 288
- B.3 Spain 291
 - B.3.1 Osera Bridge 292
 - B.3.1.1 Data Summary 292
 - B.3.1.2 Description 292
 - Further Reading 292
 - B.3.2 Llinars Del Vallès Viaduct 294
 - B.3.2.1 Data Summary 294
 - B.3.2.2 Description 294
 - Further Reading 294
 - B.3.3 Salto Del Carnero Railway Bridge, Saragossa 296
 - B.3.3.1 Data Summary 296
 - B.3.3.2 Description 296
 - Further Reading 296
 - B.3.4 Viaduct Over AP7 Riudellots de la Selva 298
 - B.3.4.1 Data Summary 298
 - B.3.4.2 Description 298
 - Further Reading 298
 - B.3.5 Contreras Bridge 300
 - B.3.5.1 Data Summary 300
 - B.3.5.2 Description 300
 - Further Reading 300
 - B.3.6 Viaduct Over River Ulla 302
 - B.3.6.1 Data Summary 302
 - B.3.6.2 Description 302
 - Further Reading 302
 - B.3.7 Almonte Bridge 304

B.3.7.1	Data Summary	304
B.3.7.2	Description	304
	Further Reading	304
B.3.8	Alcántara Bridge	306
B.3.8.1	Data Summary	306
B.3.8.2	Description	306
	Further Reading	306
B.4	Japan	309
B.4.1	Yashiro Bridge	310
B.4.1.1	Data Summary	310
B.4.1.2	Description	310
	Further Reading	310
B.4.2	Kumagawa Bridge	312
B.4.2.1	Data Summary	312
B.4.2.2	Description	312
B.4.3	Sannai-Maruyama Bridge	314
B.4.3.1	Data Summary	314
B.4.3.2	Description	314
	Further Reading	314
B.5	China	317
B.5.1	Tianxingzhou Yangtze River Bridge	318
B.5.1.1	Data Summary	318
B.5.1.2	Description	318
	Further Reading	318
B.5.2	Nanjing Dashengguan Yangtze River Bridge	320
B.5.2.1	Data Summary	320
B.5.2.2	Description	320
	Further Reading	320
B.5.3	Tongling Yangtze River Bridge	322
B.5.3.1	Data Summary	322
B.5.3.2	Description	322
	Further Reading	322
B.5.4	Beipanjiang Bridge	324
B.5.4.1	Data Summary	324
B.5.4.2	Description	324
	Further Reading	324
B.5.5	Yachihe Bridge	326
B.5.5.1	Data Summary	326
B.5.5.2	Description	326
	Further Reading	326
B.5.6	Wufengshan Yangtze River Bridge	328
B.5.6.1	Data Summary	328
B.5.6.2	Description	328
	Further Reading	328

Foreword

At the request of the authors, I have been given the honour of writing the foreword to this book, which is devoted to railway bridges. It develops the aspects referring to their structural conception, taking into account the characteristics of railway traffic: actions, limit states, speeds, etc., and includes a detailed analysis of the superstructure of the track with its different components and singular elements (for example, expansion devices) that allow the correct behaviour of the track.

In the following chapters, the knowledge and experience of the authors is passed on. In this respect, I remember a technical conference that took place in the 1970s at the Eduardo Torroja Institute, dedicated to bridges; at that time, the undersigned engineer was assigned to the Renfe Bridge Division and attended it. Ramón del Cuervo, professor of Concrete at the School of Civil Engineering in Madrid, presented a paper in which he focused on the defects and mistakes in design and execution in projects and works in which he had been involved. His presentation was the most applauded of the day's and, personally, the one from which I learned the most. I hope that reading this book will be useful to avoid the repetition of problems that can be avoided, without having to wait for experience after the execution of the works.

As the reader will appreciate, special emphasis is placed on the interactions between the structure and the track, subjected to railway and environmental actions, taking into account the requirements of their stability in different situations; solutions are also proposed and considered in relation to the transitions between the bridge and the adjacent infrastructure (and track).

Special attention is paid to the dynamic nature of railway actions, studying the dynamic response of the structure and its influence on the behaviour, also dynamic, of the track and its components, with the repercussions that this may have on safety, traffic flow quality, and maintenance needs.

To conclude, I would like to transmit here some ideas that the Emeritus Professor of Structural Engineering of the University of Berkeley, Edward L. Wilson, sets out in his book *Static and Dynamic Analysis of Structures*. In a section of Personal Remarks, he relates that his first-year physics professor warned his students 'not to use an equation they could not prove'; he also advises, with respect to modern structural

engineering, ‘not to use a structural analysis program unless you fully understand the theory and approximations contained in the program’. I fully agree with these considerations; I therefore share them with the reader, in the hope that they will be useful to them.

Madrid, June 2023

Jorge Nasarre
Civil Engineer
Caminos de Hierro Foundation

About the Authors

José Romo is Chief Executive Officer and partner of FHECOR, and also a bridge engineer fully specialised in large-span bridges with more than 40 years of experience in bridge design, 35 of them working in FHECOR. He has vast technical knowledge based on his design background complemented with his activity as professor of concrete and steel structures at Madrid University, and his active participation in national and international associations of bridge designers and concrete and steel materials. He is a member of many scientific committees such as Eurocodes, IABSE, and ACHE where he became president in 2014 and was awarded with the honour's medal in 2008. He is a fellow of the Institution of Civil Engineers of UK. He has always worked as a bridge designer participating in innumerable bridge projects in Spain and worldwide, and also in the construction engineering for many of them. He has a great aesthetic vision that he applies to all the designs, while having great concern for sustainability and the use of new materials and construction techniques.

Alejandro Pérez-Caldentey is full Associate Professor at the Department of Mechanics of Continuous Media and Theory of Structures for the Civil Engineering School at the Polytechnic University of Madrid. He joined FHECOR in 1989 after graduating from UPM where he also obtained his PhD in Civil Engineering in 1996. During his more than 34 years of experience, Alejandro has developed structural bridge projects in countries such as Spain, Chile, Italy, and the USA. He is experienced in managing multidisciplinary structural teams, developing designs, and planning and defining the scope of works. He also has extensive experience in managing and developing Research and Development projects, in Standardisation (member of the Project Team for EN 1992-1-1:2023), and in Education (Professor at UPM). He holds Engineering licenses for Spain, Chile, Virginia, Texas, Florida, North Carolina, Québec, Ontario, and British Columbia. He is also a partner and member of the Board of FHECOR Consulting Engineers.

Manuel Cuadrado holds an MSc in Civil engineering from the Polytechnic University of Madrid. He is currently Associate Professor at the Carlos III University of Madrid and a member of the Technological Committee of the Spanish Railway Research Foundation (SRRF). Manuel Cuadrado has been working for 34 years, mainly in the railway industry, for Spanish and French Engineering companies, as an independent Consultant, and from 2005 to 2017 for the SRRF. He has participated both in key Spanish High-Speed projects and in International High-Speed Lines (Portugal, Turkey, California), and has been involved in many R & D projects mainly related to the mechanical behaviour of railway infrastructures. As a result of his R & D activity, he has produced many monographs, published several papers in national and international journals, and presented many papers in national and international congresses, including WCRR 1999-Tokyo, WCRR 2001-Köln, WCRR 2006-Montreal, WCRR 2008-Seoul, and WCRR 2016-Milan, and UIC High Speed Congresses 2010-Beijing and 2015-Tokio. He was also invited to participate as a specialist in the drafting of railway standards, as a member of Spanish, European, and international technical committees. Finally, from December 2017, he has been participating as Infrastructure Assessor and Lead Assessor in several Rail Safety & Interoperability assessments, as Infrastructure expert and as Slab-track expert.

Acknowledgements

The authors would like to express their most sincere thanks to all the staff of FHECOR and the Caminos de Hierro Foundation who gave us their support and assistance in the creation and publication of this book.

We are particularly grateful to Francisco Javier Fernández Pozuelo, for his commitment and dedication to this initiative, and to Eduardo Romo for his support from the Caminos de Hierro Foundation.

The authors would like to express their deepest gratitude to Jorge Nasarre for his help in the general approach to the publication and its subsequent technical review, to Julio Sánchez for his advice and technical reviews, to Fabrice Leray for the preparation of the graphic material and the conception of the book's design, to Eduardo Conde for the layout work, and to Marta Heras for her coordination. We would also like to thank all the FHECOR engineers who prepared the High-Speed Bridge Design seminar, which was the seed of this book. Without their help and without the strong support of FHECOR and the Caminos de Hierro Foundation, this book would not have been possible. Many thanks to all of them.

of more or less length on the one hand, and bridges requiring a long main span on the other hand.

1.4.3.1 Viaducts

There are currently three types of solutions for viaducts with moderate spans and shorter or shorter lengths.

In Europe, with the exception of Germany, continuous bridges are generally built with a minimum number of structural expansion joints and corresponding track expansion joints. The deck is supported by two devices per pier and per abutment. The bridges on the US lines also generally follow these design criteria.

In China, on the other hand, isostatic solutions are being built with a complete prefabrication in one piece of the deck of each span and therefore with an expansion joint on each pier, but without track expansion joints.

As seen in Germany, semi-integral bridges are being designed and built, i.e. without pier bearings, but with structural expansion joints, and in some cases without track expansion joints.

1.4.3.2 Long-Span Bridges

The typologies being used to date are similar to road bridges. Deck trusses with variable edge have been used up to 250 m span. For longer spans (up to 450 m), arch bridges have been successfully built. For longer spans, cable-stayed bridges are the usual solution. In these cases, the decks are trussed to give greater rigidity to the system and often have two levels: the lower one for rail traffic and the upper one for road traffic.

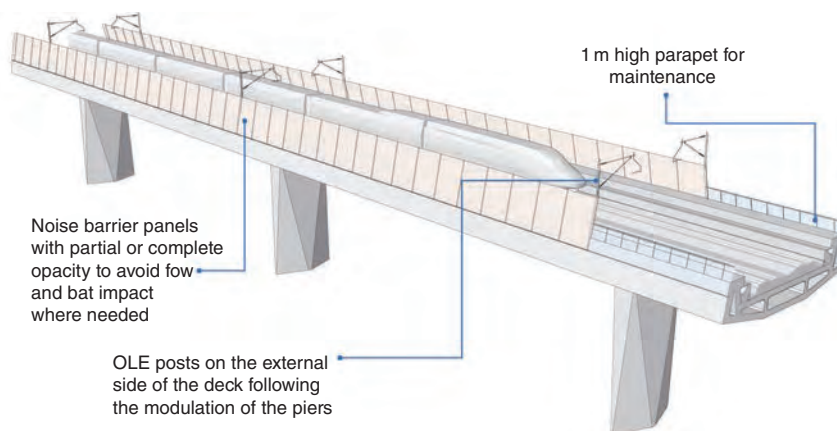
Table 1.1 summarises the bridges for high-speed lines with the longest spans built to date.

1.5 The Landscape and the Design of High-Speed Railway Bridges

1.5.1 The Traveller's Experience

The 21st century society, at least in the West, is governed by feelings [9]. The quality of any service is measured by the user experience [10]. High-speed rail is no exception to this premise.

Traditionally, when the designer analysed the engineering work and its relationship with the landscape, they did so taking into account only the view of the observer of the bridge from the surrounding environment. In this way, it is common to analyse from the different points from which the bridge or viaduct can be observed what modification it will introduce into the pre-existing landscape. The height and configuration of the abutments, the cadence of the deck spans, the relative dimensions of the deck and its spatial relationship with the morphology of the site are the aspects on which the bridge designer concerned with the landscape reflects.



What a HS2 user would see from the window of the train if a solid noise barrier is arranged (static image on the left and train running at a speed of 340 km/h on the right). Users wouldn't even notice they are crossing the Colne Valley

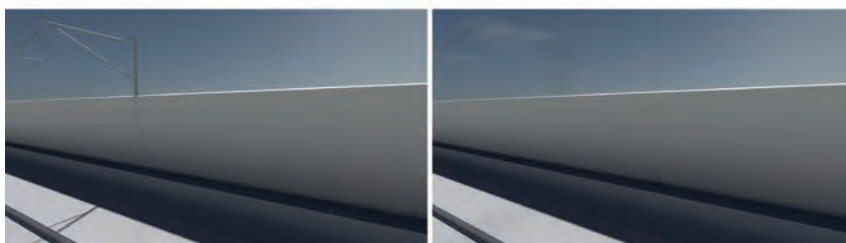


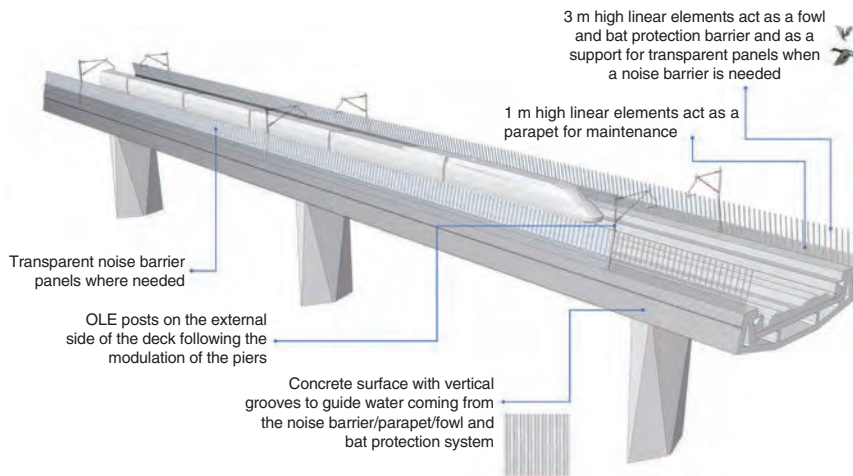
Figure 1.16 Example of a standard anti-noise panel on the bridge (Courtesy of Knight Architects).

However, it is clear that this is no longer enough. The 21st century bridge designer must also consider the landscape that the traveller will be able to contemplate when the train travels over the bridge being designed [11].

When this aspect is analysed, it is discovered that the structure itself rarely obstructs the view from the train in any way. However, it is common that parts of the bridge equipment, especially the anti-noise or wind barriers (when these are opaque), disturb or limit the view of the landscape from the train (Figure 1.16).

If the bridge is short, the loss of vision caused by such panels would only be for a few seconds. However, when the tracks run continuously through urban or peri-urban areas, the tunnel effect can be annoying or uncomfortable for the user. The same applies when the railway line passes through a point of outstanding scenic beauty, such as a major river crossing, if the passenger's view of the outside is limited by some element of the bridge.

In such cases, it will be important for the viaduct designer to be aware of whether the structure requires any type of panelling that will at least partially obstruct the vision of the traveller. Whether it is necessary to install panels or whether it is the structure itself that is disturbing, for example if the resistant section of



What a HS2 user would see from the window of the train with the transparent Specimen Design barrier (static image on the left and train running at a speed of 340 km/h on the right). At train speed, motion blur makes the vertical elements of the edge condition almost completely invisible, achieving an unobstructed view of the Colne Valley.

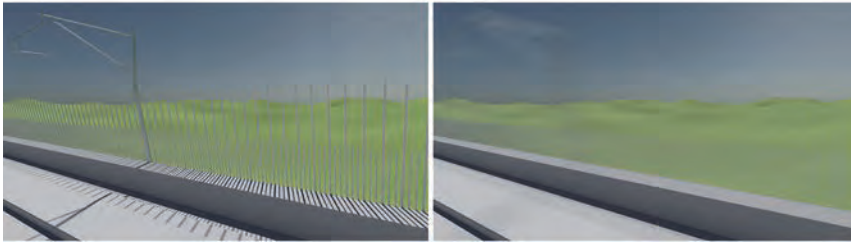


Figure 1.17 Study of the view from the train as it passes over the Colne Valley Viaduct, England, UK (Courtesy of Knight Architects).

the deck is U-shaped, the project team must analyse whether it is possible to reconcile functional requirements (noise emission control, wind safety, etc.) with the possibility of the traveller being able to enjoy the landscape at least for a fleeting glimpse (Figure 1.17).

1.5.2 The Bridge in the Landscape

The railway layouts of the 19th century and those built later for moderate traffic speeds allowed for the adaptation of the railway line to the orography, except in mountainous areas. However, compared to roads, railways have always needed more bridges and viaducts to overcome the natural obstacles they have encountered, as the layout conditions have been and still are more rigorous in the case of railways compared to the design requirements of roads.

The railway has transformed and continues to transform the landscape through which it passes. High-speed lines with their very wide radii of curvature in plan of about 8000 m minimum for 350 km/h lines require the construction of a large

number of viaducts and tunnels as soon as the terrain has some movement. Even in flat terrain, it is common for modern high-speed lines to be built in structure in order to maintain transverse territorial permeability under bridges. It is very important in these cases to decide correctly on the level of the railway grade on the ground because of its implications for the design of the viaducts.

The participation of bridge specialists in the early stages of the project is important for the definition of the basic geometry of the line and to avoid starting the project with initial conditioning factors that could damage the overall quality of the solution, for example: the transverse permeability, the landscape implications of the design, the technical quality, or the construction cost of the work.

Sections 1.5.2.1 and 1.5.2.2 analyse the landscape aspects of bridges and viaducts on high-speed lines in different scenarios.

1.5.2.1 Long Viaducts with Low Vertical Level

If the level is relatively low in relation to the ground (less than 8 m), the spans have to be short in order to leave a sufficient clearance between the bottom of the deck and the natural ground. If it is also necessary to install noise barriers, the height of the noise barrier must be added to the actual height of the deck under the track, which will make the bridge visually very heavy. One way to solve this problem is to use ‘U’ sections, with the structure itself acting as a noise barrier so that the clear span is as large as possible (Figure 1.18).

However, whenever possible, it is better to raise the level somewhat to avoid the aforementioned problems. From the point of view of the cost of the bridge, an increase in the height of the piers from 8 to 12 m has little influence on the final cost of the structure, since there will only be a slight variation in the foundations and a higher cost of the pier shafts (which in any case is a small cost in relation to the total cost of the bridge) and this increase in height will not condition the construction process of the deck. In any case, and whenever it is necessary to build either noise barriers or U-shaped structural sections, it is essential to study the shapes and finishes in order to break up the massiveness of the faces.

1.5.2.2 Long Viaducts with Medium or High Level

As explained above, when viaducts are long, it is necessary to fix the deck to the infrastructure. If the bridge is also very high, the connecting element(s) will play a special role in the formal appreciation of the bridge in the landscape.

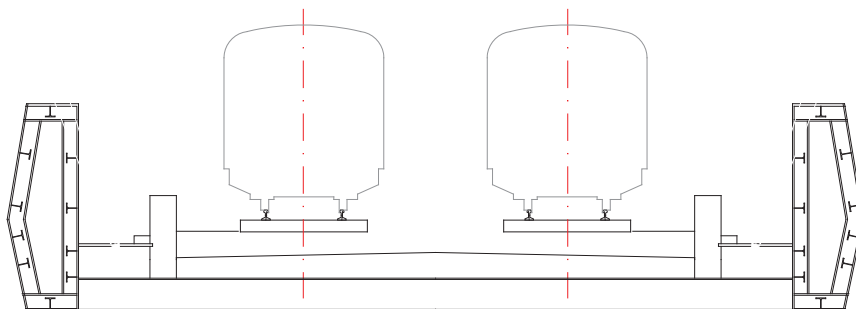


Figure 1.18 Semi-through deck structure (Source: FHECOR).



Figure 1.19 Isostatic deck, China (Courtesy of China Railways).



Figure 1.20 La Savoureuse Viaduct (2011), France (Courtesy of Wilkinson Eyre).

Isostatic Bridges When the viaduct is made up of a succession of isostatic spans, it is common for both the deck itself and the piers to be particularly robust. As the decks are isostatic, they are less efficient than continuous decks and require a greater depth (see Chapter 3). The piers also have to individually withstand the corresponding braking load and therefore require larger dimensions than in the case of continuous structures (Figure 1.19).

The La Savoureuse Viaduct (Figure 1.20) has recently been built, breaking with the French tradition of continuous bridges. In this viaduct, the piers are formed by a tetrapod-shaped structure supported at one of its vertices, which on the one hand breaks the massiveness of the piers of isostatic bridges and on the other hand reduces the span of the isostatic spans. The result is a unique structure that works well in the surrounding views.

Continuous Bridges Continuous bridges have the advantage of reducing the number of expansion joints in the structure. When these bridges are long, they require one or more points to fix the deck longitudinally.

The first example of this way of solving the central connection by means of a single element is the Pfeffetal Viaduct in Germany, 1989 (Figure 1.21). This bridge is actually an isostatic span bridge, but because of its height the piers cannot carry the braking load, which is transferred to a portal pier with two inclined piers. The shape of the V-shaped valley makes the role of this central pier very clear.



Figure 1.21 Pfeffetal Viaduct (1989), Germany (Courtesy of Wolfgang Pehlemann).



Figure 1.22 Bridge over the river Main at Gemünden (1984), Germany (Courtesy of Deutsche Bahn AG).

Another type of situation occurs when a long viaduct is required which can be resolved with modest spans, but which presents a singular span due to having to cross a major obstacle locally. This type of solution perhaps begins with the Gemünden Bridge (Figure 1.22), which serves as the cover of the most widely read book on bridge aesthetics [12].

However, to return to very long viaducts that require a single span, the revolution brought about in Germany by the Deutsche Bahn Guide [2] is worth mentioning. It stipulates that long bridges for the Deutsche Bahn should generally be semi-integral and as far as possible without a track expansion joint.

The first long bridges designed according to these guidelines are the Unstruttal (Figure 1.23) and Gänsebachtal (Figure 1.24) viaducts [3]. Both bridges are superb in terms of design, structural efficiency, maintenance of both bridge and track, as well as structural innovation, with an obvious reading on the landscape to the trained eye.

Singular Bridges Another classic design situation occurs when the obstacle to be overcome is significant and it is necessary to build at least one large span. This is a situation that occurs when crossing deep valleys or when passing over very wide and fast-flowing rivers or streams.

When crossing deep valleys, it is common for the bridge to be a short interval between tunnels. This is the case, for example, with the colossal Beipanjiang Bridge (Figure 1.25) on the high-speed line from Shanghai to Kunming in the Chinese

5.2 Methods for Dynamic Calculations and Structural Response

5.2.1 Modal Superposition

The modal superposition method can be formulated for finite elements as a function of the degrees of freedom of the structure. In this case, the eigenforms result from the analysis. Another approach, valid for simple structures is to assume a certain shape for the eigenmodes. The two approaches are developed below.

5.2.1.1 Matrix Formulation for Finite Element Analysis

The dynamic equilibrium of a system with multiple degrees of freedom (MDOF) can be written in matrix form as expressed in Eq. (5.13).

$$\mathbf{M}\ddot{\mathbf{y}} + \mathbf{C}\dot{\mathbf{y}} + \mathbf{K}\mathbf{y} = \mathbf{F}(\mathbf{t}) \quad (5.13)$$

By multiplying both sides of the equation by the inverse of the mass matrix \mathbf{M} , this equation becomes:

$$\ddot{\mathbf{y}} + \mathbf{M}^{-1}\mathbf{C}\dot{\mathbf{y}} + \mathbf{M}^{-1}\mathbf{K}\mathbf{y} = \mathbf{M}^{-1}\mathbf{F}(\mathbf{t}) \quad (5.14)$$

In most practical cases, \mathbf{M} can be assumed to be a diagonal matrix which is formed by the mass lumped at the nodes of the model. The values of the diagonal ($i = j$), M_i , would be the translational or rotational mass lumped at the node corresponding to degree of freedom i , with all other terms ($i \neq j$) being equal to 0.

Modal superposition is a simplified technique to solve the dynamic analysis of systems with n degrees of freedom (MDOF) by reducing them to solving a number m ($m \leq n$) of SDOF systems. This simplification is achieved by eigen-decomposition of matrix $\mathbf{M}^{-1}\mathbf{K}$. Φ will denote the matrix whose columns are formed by the eigenmodes.

Eigenvectors are not unique and to avoid this indeterminacy, they can be normalised, for instance, by imposing that their Euclidean norm is equal to 1.

The eigenvectors of a matrix form a base and \mathbf{y} can be expressed in terms of this base as shown in Eq. (5.15):

$$\underbrace{\mathbf{y}}_{n \cdot 1} = \underbrace{\Phi}_{n \cdot m} \underbrace{\mathbf{q}}_{m \cdot 1} \quad (5.15)$$

By introducing Eq. (5.15) into (5.13), the following expression is obtained:

$$\mathbf{M}\Phi\ddot{\mathbf{q}} + \mathbf{C}\Phi\dot{\mathbf{q}} + \mathbf{K}\Phi\mathbf{q} = \mathbf{F}(\mathbf{t}) \quad (5.16)$$

By multiplying Eq. (5.16) by the transpose of the eigenvalue matrix Φ^T , Eq. (5.17) is obtained:

$$\underbrace{\Phi^T\mathbf{M}\Phi}_{\Lambda_M = \text{diag}(M_i^*)} \ddot{\mathbf{q}} + \underbrace{\Phi^T\mathbf{C}\Phi}_{\Lambda_C = \text{diag}(C_i^*)} \dot{\mathbf{q}} + \underbrace{\Phi^T\mathbf{K}\Phi}_{\Lambda_K = \text{diag}(K_i^*)} \mathbf{q} = \Phi^T\mathbf{F}(\mathbf{t}) \quad (5.17)$$

It can be demonstrated that the eigenvectors of $\mathbf{M}^{-1}\mathbf{K}$ are orthogonal with respect to both \mathbf{M} and \mathbf{K} (for a demonstration see the Appendix of reference [3]). This makes matrices $\Phi^T\mathbf{M}\Phi$ and $\Phi^T\mathbf{K}\Phi$ diagonal.

To decouple the system of equations it is also necessary that Matrix \mathbf{C} be orthogonal with respect to Φ . This is possible by using a type of damping called Caughey damping, for which the damping matrix is expressed as a sum of powers of $\mathbf{M}^{-1}\mathbf{K}$.

$$\mathbf{C} = \mathbf{M} \sum_{i=0}^n a_i (\mathbf{M}^{-1}\mathbf{K})^i \quad (5.18)$$

This is equivalent to having a damping index for mode i equal to:

$$\xi_i = \frac{1}{2} \sum_{j=0}^{n-1} a_j (\omega_i)^{2j-1} \quad (5.19)$$

The values a_i can be determined for the system of Eq. (5.19), by imposing values of the damping index for each vibration mode.

With this assumption Eq. (5.17) becomes a series of m independent SDOF differential equations, which are easy to solve. m is the number of eigenvalues considered in the analysis. If the elements of diagonal matrix $\Lambda_{\mathbf{K}}$ are named M_i^* , the elements of diagonal matrix $\Lambda_{\mathbf{C}}$ are named C_i^* , then the expression of Eq. (5.20) holds:

$$\begin{aligned} \ddot{q}_i + \frac{C_i^*}{M_i^*} \dot{q}_i + \frac{K_i^*}{M_i^*} q_i &= \sum_{j=1}^n \frac{\phi^{-1}_{ij}}{M_i^*} F_j(t) j_y \\ C_i^* &= \Phi_i^{-1} \mathbf{C} \Phi_i \\ M_i^* &= \Phi_i^{-1} \mathbf{M} \Phi_i \\ K_i^* &= \Phi_i^{-1} \mathbf{K} \Phi_i \end{aligned} \quad (5.20)$$

In Eq. (5.20), j_y is a directional coefficient which is equal to 1.00 if force $F_j(t)$ goes in the direction of degree of freedom i and is equal to 0.00 if it does not.

The forces applied on the nodes $F_j(t)$ can be simulated by triangular pulses (Figure 5.8). The time between pulses can be approximated as the spacing between bogies, D , divided by the velocity of the train, v . The duration of the triangular pulse would be equal to the sum of the distances to the adjacent nodes divided by the velocity.

Once the independent SDOF systems have been solved, their effects need to be superimposed. This can be done, of course by direct summation of the displacements, or acceleration time histories. However, this procedure is time consuming. For this reason, it is common practice to determine the maximum response of each vibration mode at a given location and superimpose the maximum effect by using a combination rule that considers that the maximum response from the different vibration modes is not likely to occur simultaneously. A classical combination rule is the Square Root of the Sum of the Squares (SRSS), given in Eq. (5.21):

$$E = \sqrt{\sum_{j=1}^m E_j^2} \quad (5.21)$$

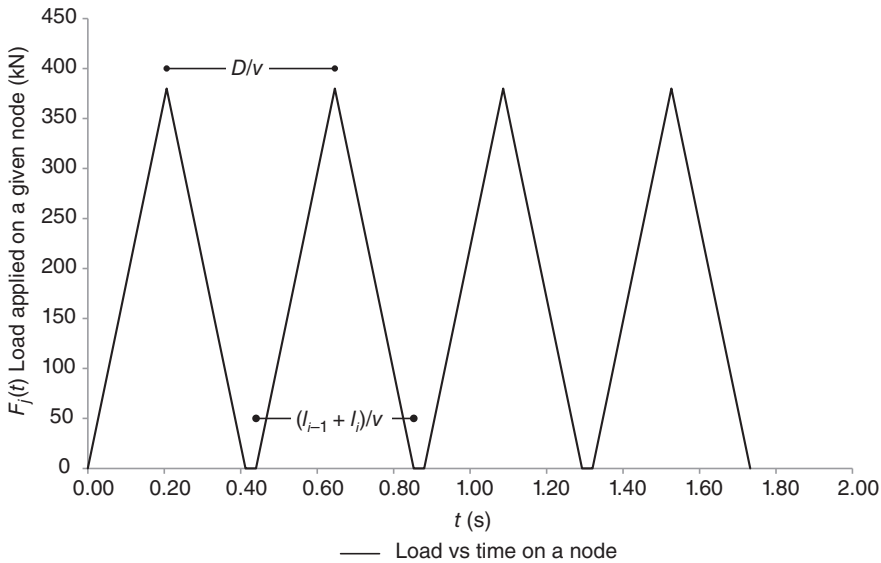


Figure 5.8 Triangular pulses simulating the train loads.

where:

E is the total estimated maximum response (displacement, acceleration, velocity) of the structure

E_j is the maximum response (displacement, acceleration, velocity) of vibration mode j .

This criterion can, however, be unsafe when the periods of the vibration modes differ by less than 10%. In such cases the Complete Quadratic Combination (CQC) should be applied. This combination criterion is defined in Eq. (5.22):

$$E = \sqrt{\sum_{k=1}^m \sum_{j=1}^m E_k r_{kj} E_j} = \sqrt{\mathbf{E}^T \mathbf{r} \mathbf{E}}$$

$$r_{kj} = \frac{8 \sqrt{\xi_k \xi_j} (\xi_k + \rho_{kj} \xi_j) \rho_{kj}^{3/2}}{(1 - \rho_{kj}^2)^2 + 4 \xi_k \xi_j \rho_{kj} (1 + \rho_{kj}^2) + 4 (\xi_k^2 + \xi_j^2) \rho_{kj}^2}$$

$$\rho_{kj} = \frac{T_k}{T_j} \leq 1 \tag{5.22}$$

This expression is very general and accounts for the possibility of having different damping indexes for the different vibration modes.

5.2.1.2 Formulation Based on Assumed Eigenforms

The formulation of Section 5.2.1.1 is the general formulation used in finite element analysis. It is also possible to formulate the problem by assuming a certain shape for the eigenforms, respecting the boundary conditions. For a simply supported beam,

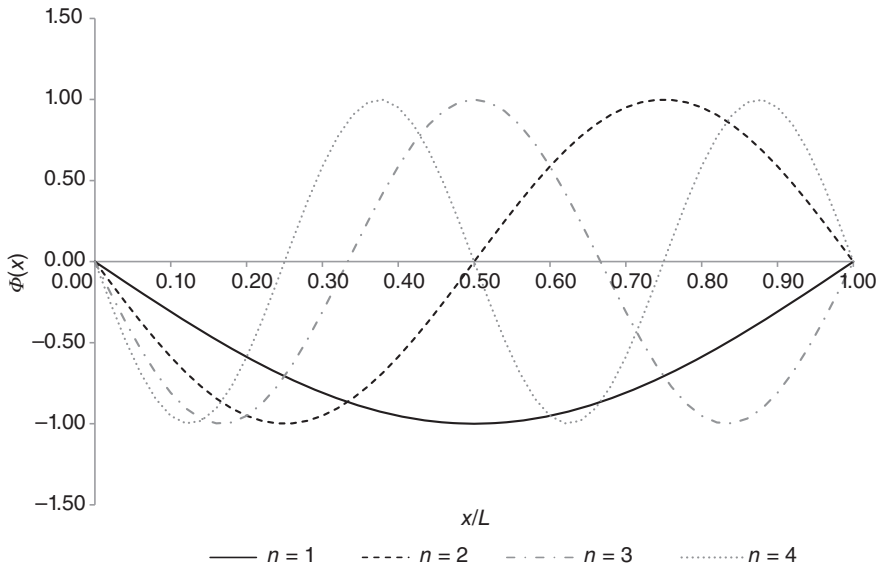


Figure 5.9 Sinusoidal eigenforms for a simply supported beam.

for example, a sine function can be adequately used to model the eigenforms (see Eq. (5.23) and Figure 5.9):

$$\phi(x) = \phi_0 \sin n \frac{\pi}{L} x \tag{5.23}$$

To maintain the criterion that the norm of the eigenforms is equal to 1.00, ϕ_0 should be fixed as follows:

$$\begin{aligned} \frac{\int_0^L \phi^2(x) dx}{L} = 1.00 &= \frac{\phi_0^2}{L} \int_0^L \sin^2 \left(n \frac{\pi}{L} x \right) dx = \frac{\phi_0^2}{2L} \int_0^L \left(1 - \cos \left(2n \frac{\pi}{L} x \right) \right) dx \\ &= \frac{\phi_0^2}{2L} \left[x - \frac{L}{2n\pi} \sin \left(2n \frac{\pi}{L} x \right) \right]_0^L = \frac{\phi_0^2}{2} = 1.00 \rightarrow \phi_0 = \sqrt{2} \end{aligned} \tag{5.24}$$

In general, to satisfy varying boundary conditions (fixed displacements or rotations), the eigenforms can take on the shape shown in Eq. (5.25) [3]:

$$\begin{aligned} \phi(x) &= a \cos \frac{n\pi}{L} x + b \sin \frac{n\pi}{L} x + c \cosh \frac{n\pi}{L} x + d \sinh \frac{n\pi}{L} x \\ \frac{\partial^4 \phi(x)}{\partial x^4} &= \underbrace{\frac{n^4 \pi^4}{L^4}}_{(a_n)^4} \phi(x) \end{aligned} \tag{5.25}$$

Note the property shown in the second line of the equation (i.e. that the fourth derivative of the eigenform with respect to x is equal to the eigenform times the fourth power of the form coefficient a_n).

An expression for the natural frequencies of the system can be determined from dynamic equilibrium conditions. It is well known from the static sectional equilibrium equation of moments that the moment is proportional to the curvature and the

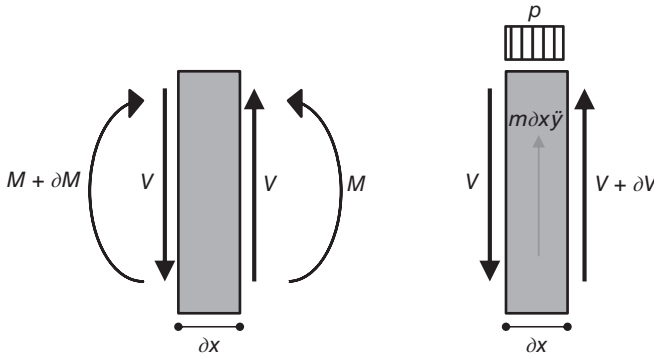


Figure 5.10 Equilibrium of a beam slice.

proportionality constant is the flexural stiffness of the section:

$$M = -EI \frac{\partial^2 y}{\partial x^2} \quad (5.26)$$

From the equilibrium conditions of a slice of a beam, it can be established that the shear force is the derivative of the bending moment and that the load per meter, p , applied on the slice minus the inertial forces is equal to the derivative of the shear force (see Figure 5.10).

$$\begin{aligned} V &= \frac{\partial M}{\partial x} = -EI \frac{\partial^3 y}{\partial x^3} \\ p - m\ddot{y} &= -\frac{\partial V}{\partial x} = EI \frac{\partial^4 y}{\partial x^4} \end{aligned} \quad (5.27)$$

Developing the second expression of Eq. (5.27), and assuming that the slice is vibrating freely, so that $p = 0$:

$$\left. \begin{aligned} m\ddot{y} + EI \frac{\partial^4 y}{\partial x^4} &= p(x, t) = 0 \\ y &= \phi(x)q(t) \\ m\phi\ddot{q} + EI \frac{\partial^4 \phi}{\partial x^4} q &= 0 \\ q(t) &= a \cos \omega t + b \sin \omega t \\ \ddot{q}(t) &= -\omega^2 q(t) \end{aligned} \right\} \rightarrow -m\phi\omega^2 q + EI \frac{\partial^4 \phi}{\partial x^4} q = 0$$

$$\rightarrow \omega^2 = \frac{EI}{m} \frac{1}{\phi} \frac{\partial^4 \phi}{\partial x^4} \rightarrow \omega = \sqrt{\frac{EI}{m} \frac{1}{\phi} \frac{\partial^4 \phi}{\partial x^4}} \quad (5.28)$$

With this approximation – i.e. assuming a shape for the eigenmodes – Eq. (5.20) can be reformulated as follows:

$$\ddot{q}_n + \frac{C_n^*}{M_n^*} \dot{q}_n + \frac{K_n^*}{M_n^*} q_n = \frac{1}{M_n^*} \int_0^L F_j(x, t) \phi_n(x) dx$$

$$C_n^* = c \int_0^L (\phi_n(x))^2 dx = cL$$

$$\begin{aligned}
 M_n^* &= m \int_0^L (\phi_n(x))^2 dx = mL \\
 K_n^* &= \frac{\partial^4 \phi}{\partial x^4} \frac{EI}{\phi_n} \int_0^L (\phi_n(x))^2 dx = \frac{\partial^4 \phi}{\partial x^4} \frac{EI}{\phi_n} L \\
 \rightarrow \ddot{q}_n + \frac{c}{m} \dot{q}_n + \underbrace{\frac{\partial^4 \phi}{\partial x^4} \frac{EI}{\phi_n m}}_{\omega^2} q_n &= \frac{1}{mL} \int_0^L F_j(x, t) \phi_n(x) dx
 \end{aligned} \tag{5.29}$$

For the case of a simply supported beam, subjected to a given generic load $F_{\max} f(\tau)$, the application of Eq. (5.29) would result in:

$$\begin{aligned}
 \phi_n &= \phi_0 \sin \frac{n\pi}{L} x \\
 \frac{\partial^4 \phi}{\partial x^4} &= \phi_0 \frac{n^4 \pi^4}{L^4} \sin \frac{n\pi}{L} x = \frac{n^4 \pi^4}{L^4} \phi_n(x) \\
 y(t) &= \phi_n(x) q_n \\
 \ddot{q}_n + \frac{c}{m} \dot{q}_n + \underbrace{\frac{n^4 \pi^4}{L^4} \frac{EI}{m}}_{\omega^2} q_n &= \frac{F_{\max}}{mL} \int_0^L f(\tau, x) \phi_n(x) dx
 \end{aligned} \tag{5.30}$$

To obtain the deflection at a given abscissa, $y(x)$, the value of $q(x)$ must be multiplied by the value of the eigenform at that coordinate so that:

$$y(x) = q(x) \phi_0 \sin \frac{n\pi x}{L} \tag{5.31}$$

Applications of this equation are given in Sections 5.2.2 and 5.2.3.

5.2.2 Response to the Isolated Load

It is straightforward to apply the formulation of Eq. (5.30) to the case of a simply supported beam subjected to a moving load. The dynamic equilibrium for the time comprised between the moment the load enters the bridge until it exits the bridge is given by Eq. (5.32). Once the load exits the bridge, the solution will be that of a damped harmonic system subjected to the initial position and velocity conditions present at the time the load exits the bridge.

$$\begin{aligned}
 \ddot{q}_n(x) + \frac{c}{m} \dot{q}_n(x) + \underbrace{\frac{n^4 \pi^4}{L^4} \frac{EI}{m}}_{\omega^2} q_n(x) &= \frac{P}{mL} \int_0^L f(\tau, x) \phi_n(x) dx \\
 f(\tau, x) = \delta(x - vt) &\rightarrow \int_0^L \delta(x - vt) \phi_n(x) dx = \phi_n(vt) \\
 \ddot{q}_n(x) + \frac{c}{m} \dot{q}_n(x) + \omega^2 q_n(x) &= \frac{P}{mL} \phi_0 \sin \left(\underbrace{\frac{n\pi}{L} vt}_{\omega_f t} \right)
 \end{aligned} \tag{5.32}$$

$\delta(x)$ in Eq. (5.32) is Dirac's delta function which is equal to infinity when $x = 0$ and equal to 0 otherwise. It has the property shown in Eq. (5.33):

$$\int \delta(x - a)f(x)dx = f(a) \quad (5.33)$$

The problem of Eq. (5.32) is in fact the same problem of forced vibrations solved in Appendix A. However, in this case, damping is accounted for. It can be verified that the sum of a sine function plus a cosine function with natural frequency equal to ω_f is a particular solution of Eq. (5.32). The full solution to the equation will be the sum of the particular solution and the general solution to the homogenous equation (damping is ignored here for the part of the solution corresponding to forced vibration, since it will be neglectable, for typical bridge damping ratios, because of its short duration):

$$\begin{aligned} q &= A \cos \omega_f t + B \sin \omega_f t + e^{-\xi \omega t} (C \cos \omega_d t + D \sin \omega_d t) \\ \dot{q} &= -A \omega_f \sin \omega_f t + B \omega_f \cos \omega_f t - \xi \omega e^{-\xi \omega t} (C \cos \omega_d t + D \sin \omega_d t) \\ &\quad + \omega_d e^{-\xi \omega t} (-C \sin \omega_d t + D \cos \omega_d t) \\ \ddot{q} &= -A \omega_f^2 \cos \omega_f t - B \omega_f^2 \sin \omega_f t + \xi^2 \omega^2 e^{-\xi \omega t} (C \cos \omega_d t + D \sin \omega_d t) \\ &\quad - \xi \omega_d \omega e^{-\xi \omega t} (-C \sin \omega_d t + D \cos \omega_d t) - \xi \omega_d \omega e^{-\xi \omega t} (-C \sin \omega_d t + D \cos \omega_d t) \\ &\quad - \omega_d^2 e^{-\xi \omega t} (C \cos \omega_d t + D \sin \omega_d t) \\ \ddot{q}_n(x) + 2\xi \omega \dot{q}_n(x) + \omega^2 q_n(x) &= \frac{P}{m} \phi_0 \sin \omega_f t \end{aligned} \quad (5.34)$$

The values of A and B can be identified by imposing that the terms in $\cos \omega_f t$ and $\sin \omega_f t$ must cancel out, as shown in Eq. (5.35)

$$\left\{ \begin{array}{l} A \left(\omega^2 - \omega_f^2 \right) + B \frac{2\xi m \omega}{m} \omega_f = 0 \\ -A \frac{c}{m} \omega_f + B \left(\omega^2 - \omega_f^2 \right) = \phi_0 \frac{P}{m} \end{array} \right. \rightarrow \left\{ \begin{array}{l} A = \phi_0 \frac{P}{m} \frac{-2\xi \omega \omega_f}{\left(\omega^2 - \omega_f^2 \right)^2 + 4\xi^2 \omega^2 \omega_f^2} \\ B = \phi_0 \frac{P}{m} \frac{\left(\omega^2 - \omega_f^2 \right)}{\left(\omega^2 - \omega_f^2 \right)^2 + 4\xi^2 \omega^2 \omega_f^2} \end{array} \right. \quad (5.35)$$

The values of coefficients C and D can then be determined from the initial conditions of a system that is initially at rest:

$$\begin{aligned} q(0) = 0 = A + C &= \frac{-2\xi \omega \omega_f \phi_0 \frac{P}{m}}{\left(\omega^2 - \omega_f^2 \right)^2 + 4\xi^2 \omega^2 \omega_f^2} + C \\ \rightarrow C &= \frac{2\xi \omega \omega_f \phi_0 \frac{P}{m}}{\left(\omega^2 - \omega_f^2 \right)^2 + 4\xi^2 \omega^2 \omega_f^2} \\ \rightarrow C &= \phi_0 \frac{P}{m} \frac{2\xi \omega \omega_f}{\left(\omega^2 - \omega_f^2 \right)^2 + 4\xi^2 \omega^2 \omega_f^2} \\ \dot{q}(0) = 0 = B \omega_f - \xi \omega C + \omega_d D \end{aligned}$$

$$\begin{aligned}
 \rightarrow D &= -\frac{(\omega^2 - \omega_f^2) \phi_0 \frac{P}{m} \omega_f}{(\omega^2 - \omega_f^2)^2 + 4\xi^2 \omega^2 \omega_f^2} \frac{\omega_f}{\omega_d} + \xi \frac{\omega}{\omega_d} \frac{2\xi \omega \omega_f \phi_0 \frac{P}{m}}{(\omega^2 - \omega_f^2)^2 + 4\xi^2 \omega^2 \omega_f^2} \\
 \rightarrow D &= \phi_0 \frac{P}{m} \frac{\frac{\omega_f}{\omega_d} (2\xi^2 \omega^2 - (\omega^2 - \omega_f^2))}{(\omega^2 - \omega_f^2)^2 + 4\xi^2 \omega^2 \omega_f^2}
 \end{aligned} \tag{5.36}$$

The position and velocity of the structure can be determined when the force exits the structure as follows:

$$\begin{aligned}
 q_0 &= \frac{\phi_0 P}{m(\omega^2 - \omega_f^2)^2 + 4\xi^2 \omega^2 \omega_f^2} \\
 &\quad \cdot \left(\begin{aligned} &-2\xi \omega \omega_f \cos \omega_f \frac{L}{v} + (\omega^2 - \omega_f^2) \sin \omega_f \frac{L}{v} \\ &+ e^{-\xi \omega \frac{L}{v}} \left(2\xi \omega \omega_f \cos \omega_d \frac{L}{v} + \frac{\omega_f}{\omega_d} (\omega^2 - \omega_f^2) \sin \omega_f \frac{L}{v} \right) \end{aligned} \right) \\
 \dot{q}_0 &= \frac{\phi_0 P}{m(\omega^2 - \omega_f^2)^2 + 4\xi^2 \omega^2 \omega_f^2} \\
 &\quad \cdot \left(\begin{aligned} &2\xi \omega \omega_f^2 \sin \omega_f \frac{L}{v} + \omega_f (\omega^2 - \omega_f^2) \cos \omega_f \frac{L}{v} \\ &- \xi \omega e^{-\xi \omega \frac{L}{v}} \left(\begin{aligned} &2\xi \omega \omega_f \cos \omega_d \frac{L}{v} \\ &+ \frac{\omega_f}{\omega_d} (2\xi^2 \omega^2 - (\omega^2 - \omega_f^2)) \sin \omega_d \frac{L}{v} \end{aligned} \right) \\ &+ \omega_d e^{-\xi \omega \frac{L}{v}} \left(\begin{aligned} &-2\xi \omega \omega_f \sin \omega_d \frac{L}{v} \\ &+ \frac{\omega_f}{\omega_d} (2\xi^2 \omega^2 - (\omega^2 - \omega_f^2)) \cos \omega_d \frac{L}{v} \end{aligned} \right) \end{aligned} \right)
 \end{aligned} \tag{5.37}$$

The above equations can be applied for the number of eigenmodes considered. To obtain the actual displacements, the generalised coordinates q , should be multiplied by the value of the eigenmode at the given location (see Eq. (5.31)). Therefore, the contribution to the deflection at centre span for pair values of n will be nil.

To see an application of this method, the same example already analysed in Section 5.1.4 is considered. The example consists in a simply supported bridge with a span, L , of 4500 m. The area of the section is 7.96 m² and the inertia 7.71 m⁴. The elastic modulus of concrete is taken as 36.2 GPa. Additionally, an upper-bound superimposed dead load equivalent to $G_{2,\text{sup}} = 137.6$ kN/m is present. So, the total upper-bound mass of the structure is $M = (7.96 \cdot 2.5 + 13.76) \cdot 45 = 1514.7$ ton. The first natural period of this structure is $T1 = 0.448$ s. It is assumed that the train is a high-speed train, and that the maximum velocity is 350 km/h (i.e., $v \sim 100$ m/s) and that the damping index is 1% as recommended by EN 1991-2 (see Table 5.3).

Figure 5.11 shows the response of the system in terms of maximum deflection at centre span for the first four modes of vibration. It is very clear that in such a

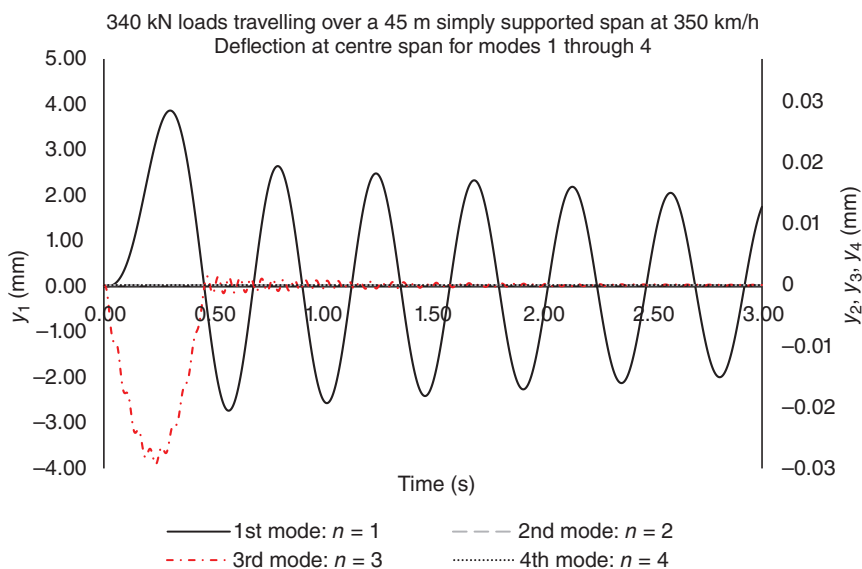


Figure 5.11 Deflections due to the first four vibration modes – plotted separately.

system, only the first mode of vibration is of significance (note that the deflection of modes 2, 3, and 4 is plotted on the secondary axis on a different scale, roughly 100 times larger). Modes with pair values of n do not contribute at all to the deflection at centre span since the deflection of the corresponding eigenmodes is nil at that point. Figure 5.12 shows the deflection due to the superposition of the first four modes compared to that of the first model only. The maximum deflection of the superposed modes is 0.64% lower than that of the first mode only and the difference can barely be seen.

Table 5.4 shows the natural frequencies of the first four modes, the maximum centre span deflection due to each mode, the deflection due to the sum of the modes and the deflection obtained by the SRSS criterion, which would be applicable since the difference between the periods of the first four modes is much larger than 10%. The SRSS criterion is safe sided for this case since the contribution of the third mode is negative at centre span.

Table 5.4 Maximum deflection in the structure [mm].

Mode	1	2	3	4		
ω (rad/s)	14.03	56.14	126.31	224.55		
T (s)	0.448	0.112	0.050	0.028	Sum (mm)	SRSS (mm)
Deflection (mm)	3.815	0.000	-0.029	0.000	3.790	3.815

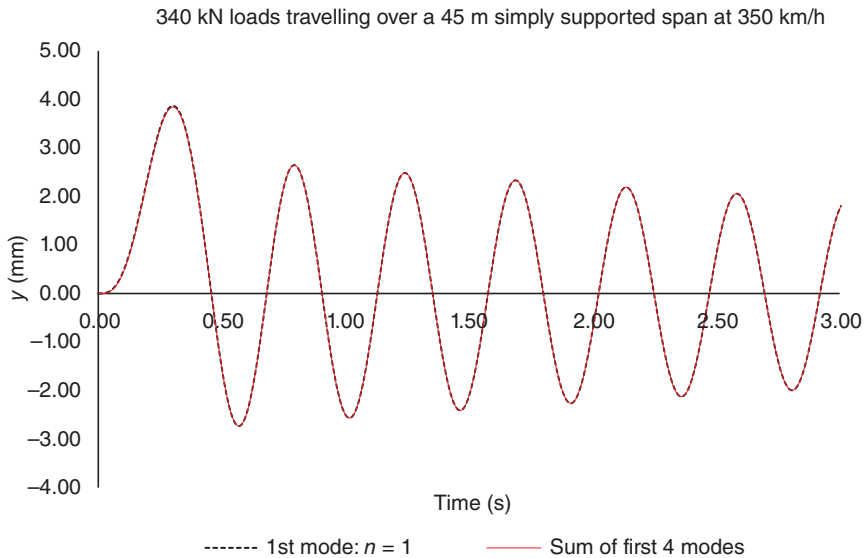


Figure 5.12 Deflections due to the additive effect of the first four vibration modes.

5.2.3 Response to the Train Loads

The response to the train load can be computed by superposing the effect of a number N of axes with a time delay equal to the distance between bogies, D , divided by the velocity of the train. In the case of the train load, the maximum response is not obtained for the fastest train passage but for a time between loads equal to the natural period of the structure. The following figures have been obtained by applying this methodology to the example considered in Section 5.1.4. In this case the natural period is 0.448 s. 14 bogies carrying a total load of 340 kN each, and spaced 22 m apart, are traveling at a velocity equal to $22/0.448 = 49.1$ m/s (176.8 km/h). The damping index ξ is assumed to be 1%. As a simplification, which is justified by the results shown in Section 5.2.2, only the first vibration mode will be considered here. Figure 5.13 shows the individual effect on the bridge deflections of the passage of the first 4 bogies. The vibrations once the train leaves the structure are in synchronicity.

Figure 5.14 shows the superposition of the passage 7 and 14 bogies, compared to the effect of one bogie, in terms of maximum deflection. A clear resonant effect can be seen. The deflection increases with time, until the last bogie leaves the deck, after which moment the maximum deflection goes down as only the vibrations left over from the passage of the 14 bogies are active. These vibrations gradually decrease due to damping.

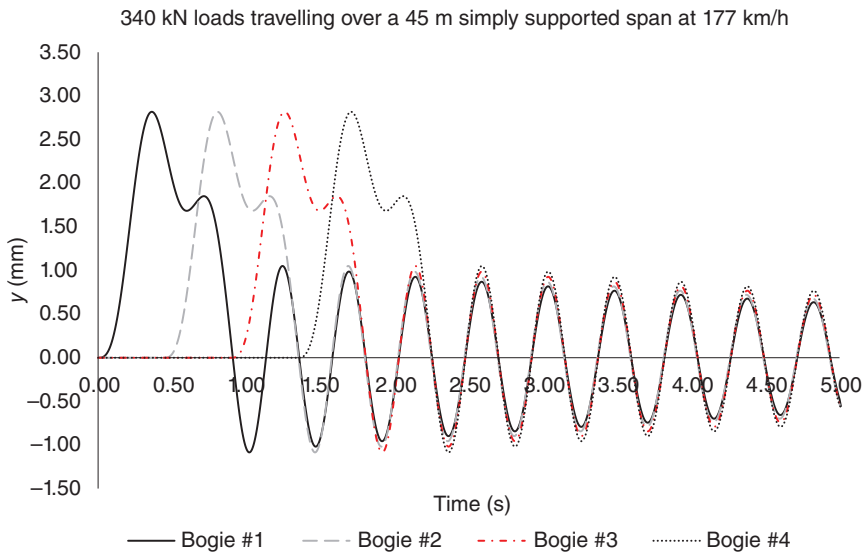


Figure 5.13 Effect of individual loads.

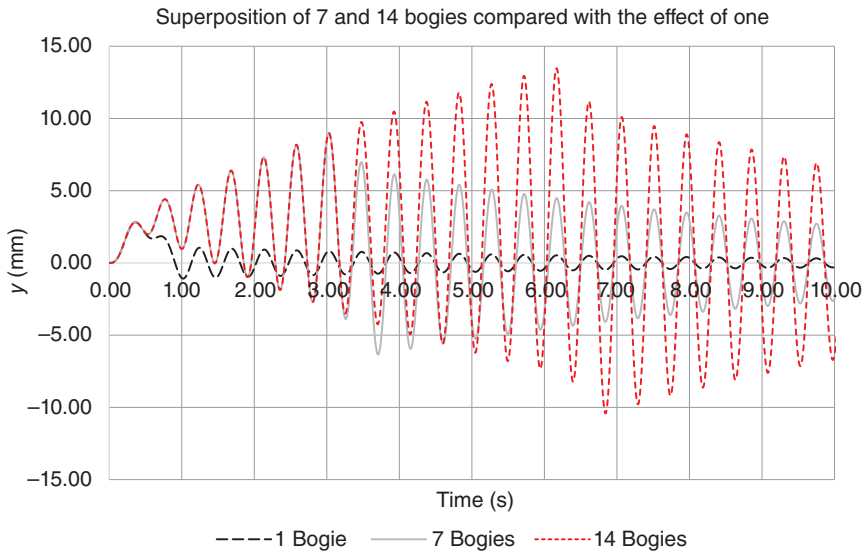


Figure 5.14 Superposition of several bogies.

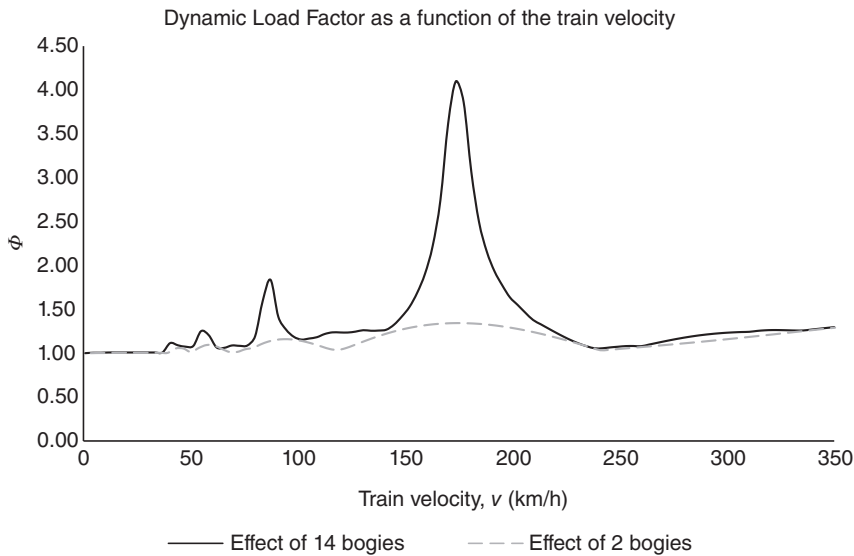


Figure 5.15 Dynamic Load Factor (ϕ) as a function of the train velocity.

Figure 5.15 shows the Dynamic Load Factor as a function of the train velocity. A very clear resonant peak can be observed at 177 km/h (corresponding to the first natural period of vibration).¹ Also shown in the figure is the effect of two bogies (which is the maximum number that will be on the bridge at a given time). With only two bogies, there is no resonant phenomenon and, in this case the response increases with the velocity of the train. This is logical as more energy is transferred to the structure and the ratio between the load duration and the natural period of the structure is not too low ($t_d/T \sim 0.5$ for a velocity of 350 km/h).

5.2.4 Effect of Damping

In real structures damping values are low (going from 0.5–1% for steel decks to 2% for concrete decks). These values are not very significant for individual loads. However, when train load is considered, the time lapse between the passage of the successive bogies provides some room for action by damping. Even with these low damping indexes the effect is quite significant. Figure 5.16 shows how the Dynamic Load

¹ It is interesting to note that for such a speed, a dynamic analysis would not be required by EN 1991-2:2003, despite the fact that resonance occurs. In this case, the Dynamic Load Factor estimated according to Eq. (5.3) would be only 1.03. However, this factor is applied to the LM71 or SW/0, SW/2 trains which are much heavier than the real trains. For the LM71 train, the maximum static deflection would be 18.6 mm, much larger than the 13.44 mm of the real train accounting for the dynamic behaviour. This comparison demonstrates that such cases are covered by the envelope loading.

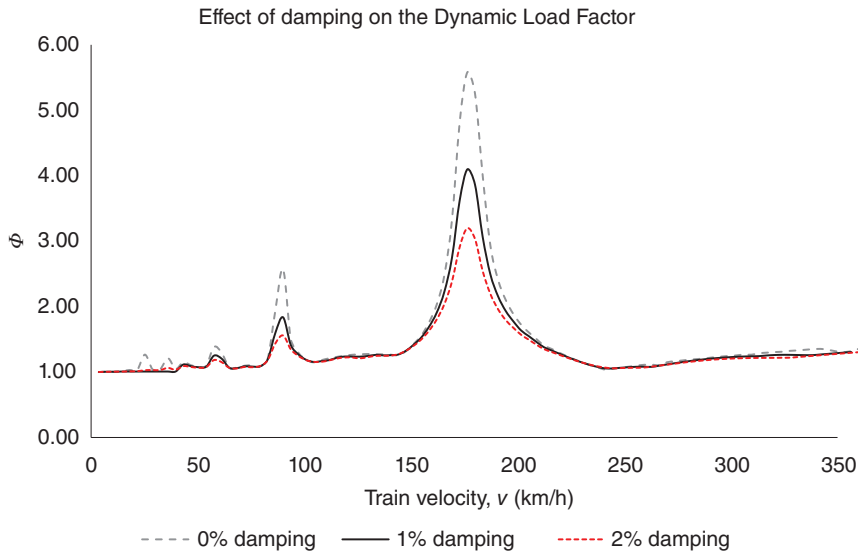


Figure 5.16 Effect of damping on Dynamic Load Factor.

Factor varies when there is no damping compared to 1% and 2% damping indexes. For the peak response, Φ increases from 3.2 for a 2% damping index to close to 5.6 if damping is not accounted for.

5.2.5 Dynamic Interaction Between Vehicle and Structure

The interaction between vehicle and structure normally has a favourable effect on the dynamic behaviour of railway bridges. According to [4], its effects are most noticeable in simply supported bridges with small spans and low damping. In these cases, the reduction in accelerations and displacements at resonance can reach 30%.

There are several levels for the modelling of the interaction between vehicle and structure. The most sophisticated models consider not only the interaction between vehicle and structure but also the interaction with the track, in which rails, sleepers, and ballast are all considered (see Figure 5.17). Such models, however, are too complex and are more useful for research than for practical applications.

A second-level approximation, which has been applied in practice, considers the modelling of each vehicle with two bogies, and represents the connection between car and bogie and the connection between bogie and each axle (see Figure 5.18). In this case the body of the vehicle is assigned a mass (M) and a rotational inertia (J). The vehicle is connected, though secondary suspension (modelled by a spring $-K_s$ - plus a damper $-C_s$ - placed in parallel), to the bogie frame which is also assigned a mass (M_B) and a rotational inertia (J_B). Each axle is connected to the bogie frame by

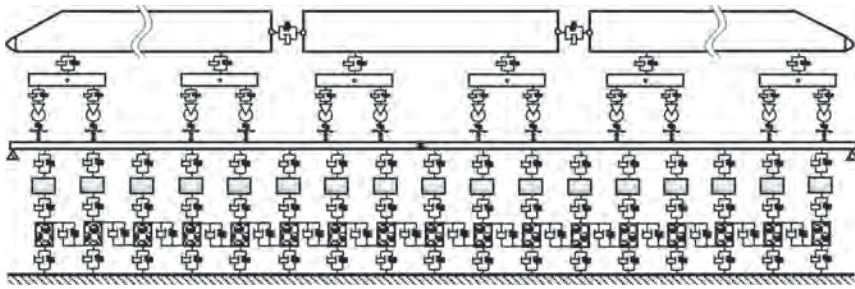


Figure 5.17 Dynamic interaction model considering the interaction between vehicle, track, and structure [5].

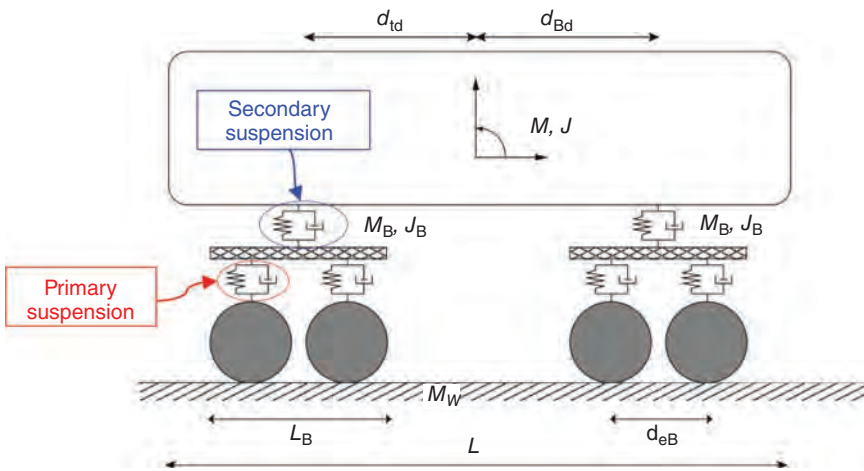


Figure 5.18 Full vehicle-structure interaction model (Source: taken from [4]).

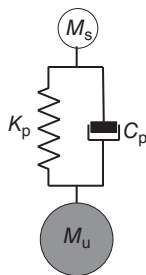


Figure 5.19 Simplified model to account for vehicle-structure interaction.

secondary suspension modelled as a coupled spring/damper pair (K_p/C_p) for each axle. Finally, the mass of the wheels (M_w) is applied directly on the structure.

There are also simplified models in which the axles are considered as independent elements and only primary suspension is considered. Each one can be modelled as shown in Figure 5.19. In this case M_s corresponds to the suspended mass

B.3.5 Contreras Bridge

B.3.5.1 Data Summary

Owner	ADIF
Place	Contreras Reservoir, Spain
HSR Line	Madrid – Levante
Designer	Carlos Fernández Casado CFC
Contractor	AZVI-Contractora San José
Main span	261 m
Deck Width	14.20 m
Length	587 m
Deck type	Continuous box girder
Material	Concrete
Typology	Arch
Start construction	2007
Completion	2009

B.3.5.2 Description

The arch, with a span of 261 m, was divided into six parts by vertical columns. The arch follows a polygonal guideline. The antifunicular of the arch is perfect in this way, reducing the deflections that would exist in the area between the vertical columns if the arch were perfectly curved.

It is a reinforced concrete arch bridge with a continuous prestressed concrete box deck and two access viaducts. The span of the arch is 261 m and a rise at the centre is 36.95 m, and therefore a rise -to-span ratio of 1/6.77.

Further Reading

- Manterola, J., Martínez, A., Navarro, J.A., et al. (2008): Puente de ferrocarril de alta velocidad sobre el embalse de Contreras. *Presented at: IV Congreso ACHE*, Valencia.
- Manterola, J., Martínez, A., Navarro, J.A., and Martín, B. (2012). Puente arco de ferrocarril sobre el embalse de Contreras en la línea de alta velocidad Madrid-Levante. *Revista Hormigón y Acero* 63 (264).



Figure B.33 Contreras Bridge (Courtesy of Carlos Fernández Casado CFC & ADIF).



Figure B.34 Contreras Bridge (Courtesy of Carlos Fernández Casado CFC & ADIF).

B.3.6 Viaduct Over River Ulla

B.3.6.1 Data Summary

Owner	ADIF
Place	Catoira, Spain
HSR Line	Atlantic Axis Pontevedra – La Coruña
Designer	IDEAM
Main span	240 m
Contractor	DRAGADOS-TECSA
Deck Width	14 m
Length	1620 m
Deck type	Continuous composite deck
Material	Steel
Typology	Steel Truss
Start construction	2011
Completion	2015

B.3.6.2 Description

The viaduct over the river Ulla where it flows into the Arosa Estuary. The design minimises the number of piers on the course of the river and tries to seek the maximum transparency and the minimum visual impact possible on the surrounding landscape. The bridge is a composite variable depth structure with three large central spans over the water measuring 225 + 240 + 225 m and 120 m access spans. The deck has a variable depth with 17.90 m on the piers section and 9.15 m at the centre of the span. This depth remains constant on the access spans. The four main piers were reinforced to resist deck rotation and control the level flexion transmitted to the foundations through the frame effect, thus preventing over-sizing. For this reason, the main piers located at the outer edges of the 225 m spans were designed with two free-standing partitions driving into the foundations and pier capitals. The remaining piers are conventional. The deck support over these piers is free spherical lengthwise bearings. The track has expansion joints coinciding with the expansion structural joint in the abutments.

Further Reading

- Millanes, F., Ortega, M., and Matute, L. (2014). Viaduct over river Ulla: an outstanding composite (steel and concrete) high-speed railway viaduct. *Structural Engineering International* 24.
- Millanes, F., Ortega, M., and Estévez, R. (2015). Viaduct over Ulla River in the Atlantic high-speed railway line: A composite (steel–concrete) truss world record. (ACHE, ELSERVIER, Hormigón y Acero 66(277)).



Figure B.35 Ulla River Viaduct (Courtesy of ADIF).



Figure B.36 Ulla River Viaduct (Courtesy of ADIF).

B.3.7 Almonte Bridge

B.3.7.1 Data Summary

Owner	ADIF
Place	Almonte River, Cáceres, Spain
HSR Line	Madrid – Extremadura – Portuguese border
Designer	Arenas y Asociados
Contractor	FCC Fomento de Construcciones y Contratas
Main span	384 m
Deck Width	14.2 m
Length	996 m
Deck type	Continuous box girder
Material	Concrete
Typology	Arch
Start construction	2011
Completion	2016

B.3.7.2 Description

The bridge has a large concrete arch with an upper deck spanning 384 m over the Alcantara reservoir. This large arch is the main element of a 996 m long viaduct, consisting of 12 approach spans with 45 m spans, and two additional spans of 36 m at the ends.

The deck has a prestressed concrete box section with a constant 3.1 m depth. The viaduct piers have a maximum height of 65.3 m. Both those found at ground and those supported on the arch have a variable octagonal cross-section, the aerodynamics of which are beneficial for the arch span, given its large span. Almonte's main mechanism for taking the longitudinal forces from trains braking is the fixed point located at the apex of the arch. At the centre of the bridge there is a 42 m long fixed point connecting the arch and the deck. Horizontal braking loads are transferred through the fixed point from the deck to the arch and then into the abutments. All the columns are connected to the deck with bearings, allowing the deck to move longitudinally with respect to the columns.

Further Reading

- Arenas, J.J., Capellán, G., Martínez, J. et al. (2016). Viaduct over River Almonte. Design and Analysis. In: *Presented at: IABSE Symposium: Challenges in Design and Construction of an Innovative and Sustainable Built Environment*, Stockholm, Sweden.
- Capellán, M. (2015). Puente arco de alta velocidad sobre el río Almonte. ROP Revista de Obras Públicas n° 3562 Madrid. Spain.



Figure B.37 Almonte Bridge (Courtesy of Arenas Asociados & ADIF).



Figure B.38 Almonte Bridge (Courtesy of Arenas Asociados & ADIF).